Experimental Investigation of a Downwind Coned Wind Turbine Rotor under Yawed Conditions: Preliminary Results

IOP Conf. Series: Journal of Physics: Conf. Series **1356** (2019) 012018 doi:10.1088/1742-6596/1356/1/012018

Experimental Investigation of a Downwind Coned Wind Turbine Rotor under Yawed Conditions: Preliminary Results

C W Schulz, K Wieczorek, S Netzband, M Abdel-Maksoud

Hamburg University of Technology, 21073 Hamburg, Germany

christian.schulz@tuhh.de

Abstract. The growing number of Floating Offshore Wind Turbine (FOWT) concepts that utilize a single point mooring and therefore rely on the self-alignment capabilities of the wind turbine (e.g. SCD nezzy or SelfAligner by CRUSE Offshore) demands an extension of the simulation methods used for their development. A crucial issue for these concepts is the accurate prediction of forces and moments, which contribute to the self-alignment. In contrast to the well-studied behaviour of torque and thrust, yaw moment and lateral forces on a rotor under yawed conditions have not been in focus of previous experimental tests for the validation of aerodynamic simulation tools. In the present work, a model turbine equipped with a 6-axis force/moment sensor to capture the complete load on the rotor is presented. A detailed study of the two-bladed model turbine's aerodynamic behaviour under yawed conditions was carried out within a range of yaw angles between -55 to + 55° with steps of 1 – 2.5°.

1. Introduction

The large number of recently erected prototypes and funded demonstration projects in the field of floating offshore wind turbines worldwide shows the extent to which governments and the industry are interested in this technology. Two key aspects are the reason for this interest: The low dependency of costs on water depth and the potentially easier installation procedure in comparison to bottom-fixed offshore wind turbines. Most current designs utilize a conventional offshore wind turbine mounted on an individually designed floating platform like the Hywind Spar[1] or the Floatgen Demonstrator[2]. Another approach makes use of the floating platform`s manoeuvrability instead of a yaw bearing at the tower top to align the rotor with the wind. Several concepts of these self-aligning floating wind turbines were presented in the past (eg. SCD nezzy[3], HEXICON[4], EOLINK[5] or SelfAligner[6] by CRUSE Offshore. The main engineering challenge in this case is to maintain a proper alignment of rotor and wind direction even in unfavourable environmental conditions like wind-wave or wind-current misalignment. Therefore, in addition to power and thrust, yaw moment and lateral force of the wind turbine rotor in a wide range of yaw angles need to be predicted accurately in the design process. In

[1] http://www.equinor.com/en/what-we-do/hywind-where-the-wind-takes-us.html
[2] http://www.ideol-offshore.com/en/floatgen-demonstrator
[3] http://www.scd-technology.com/scd-technology-scd-nezzy/
[4] http://www.hexicon.eu/
[5] http://www.eolink.fr/
[6] http://www.cruse-offshore.de/

contrast to this need, conventionally used blade element momentum theory based methods and also more complex methods have not been validated with respect to these requirements, as a detailed set of validation data has not been published until now.

In order to provide such validation data, an experimental measurement campaign with close attention to the rotor yaw moment was conducted in the wind tunnel of the Hamburg University of Technology (TUHH). The forces and moments acting on a two-bladed rotor with a downwind cone angle of 5° were studied in a range between -55 and 55°. This paper presents an overview on the setup of the model test, the design and the manufacturing of the model turbine as well as an analysis of the results of the measurement campaign. The scientific context of previous experiments is given in the following section.

2. Previous investigations

A considerable number of wind turbine experiments in a wind tunnel environment under yawed conditions were conducted in the past 40 years. However, only a few of them paid attention to the yaw moment. Micallef and Sant give an overview of the research activities and most of the relevant experimental studies in this field going back to 1982 in [1]. Most of the earlier studies analysed the flow field in the wake in order to understand the physics of a yawed inflow. Consequently, only a few investigations monitored the loads on the rotor. Two of them are the well-known Nasa-Ames and MEXICO experiments, which are unique in terms of their small scaling ratio and the elaborate testing methodology. The blade root of the both turbines were equipped with strain gauges [2][3], which were used to measure the blade loads as well as torque and yaw moment. Alternatively, torque, thrust and yaw moment could be computed based on the surface pressure at different blade sections that were recorded using a high number of pressure sensors on the blade surface. Furthermore, Maeda et al. [4] conducted an experimental study using a model turbine with 2.4 m rotor diameter that focused on measurements of the blade pressure but additionally recorded the torque using an unspecified ‘torque meter’. Thrust and yaw moment could therefore be obtained from the local blade pressure measurements but were not computed or published for this experiment. Krogstad and Adaramola [5] also utilized a torque sensor integrated in the shaft of their model turbine with 0.9 m rotor diameter. Additionally, a six-component balance located below the wind tunnel floor was used to measure the thrust force. An additional test was carried out without the blades to investigate the contribution of the drag force acting on the comparatively large tower and nacelle on the thrust force and the results were used to correct the thrust. The yaw moment can also be measured using the six-component balance but strong deviations due to tower and nacelle drag force need to be taken into account.

Considering the above-mentioned studies only the Nasa-Ames and the MEXICO experiment deliver reliable data for the absolute yaw moment. During the tests at Nasa-Ames a moderate downwind cone angle of 3.4° was applied to the rotor. Measurements at 0°, 10°, 20°, 45° and 90° yaw angle were conducted and therefore a coarse picture of power, thrust and yaw moment of a downwind coned rotor could be drawn from the measurements. However, to the authors’ best knowledge an investigation focussing on the yaw moment has not been published in the past. Two different cone angles in upwind and downwind configuration were considered in water tank experiments by Kress et al. [6]. Similar to the present work, special attention was paid on the yaw moment, which was investigated at -10°, 0° and 10°. In addition to the cone angle, a tilt angle of 8° was applied in order to account for its effect on the yaw moment simultaneously.

Downwind coned rotors are expected to deliver a higher stabilising yaw moment in comparison to non-coned or upwind coned rotors. Fundamental research on downwind turbines has been published in the past [7], but as described above, experimental investigations with regard to the yaw moment of downwind coned rotors are sparse. Therefore, the present investigation aims at providing validation data to allow a deeper understanding of the underlying effects in the future.

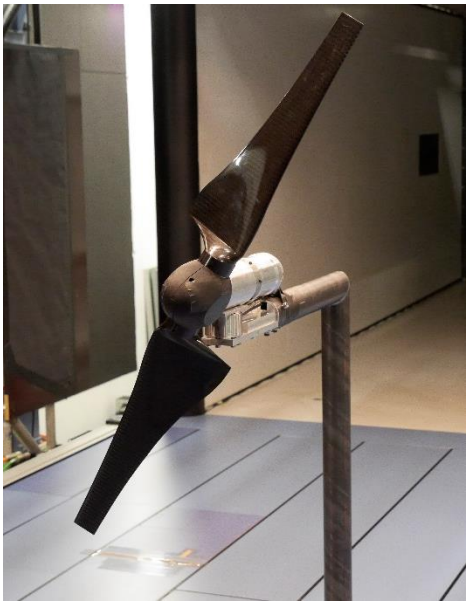

Figure 1: Wind turbine model.

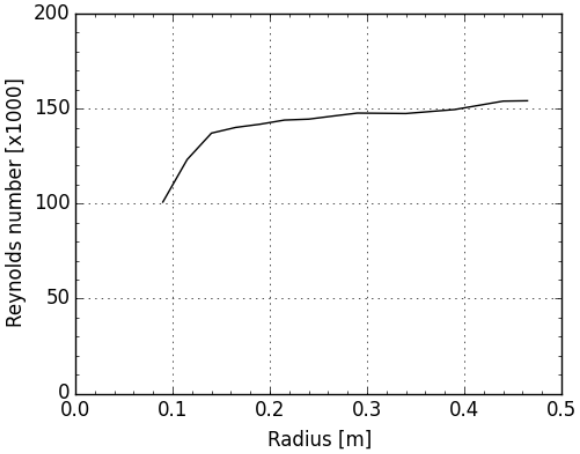

Figure 2: Local Reynolds number at the blade over rotor radius.

3. Experimental setup

The model tests were conducted in the wind tunnel of the Hamburg University of Technology with a test section of 2 m in height and 3 m in width. In order to keep blockage effects on the measurements small, a rotor diameter of 0.925 m and a comparatively low blockage ratio of 11.2 % were chosen. Extreme values for the blockage are 17.6 % for the MEXICO rotor where blockage effects were present but limited [8] and 8.8 % for the NASA-Ames Experiment where blockage effects were found to be negligible [9][10]. Following Krogstad and Lund [11], it is assumed that a blockage ratio slightly higher than in the NASA-Ames experiment will still have very limited influence on the measured quantities at moderate thrust coefficients. The downwind cone angle of 5° was applied to achieve a high yaw moment while staying within the limitations of a realistic commercial design. A two bladed configuration was used instead of a three-bladed, which leads to a higher local chord length and therefore to a higher local Reynolds number at the blade sections.

The blade design was driven by a low sensitivity to changes in the Reynolds number and a high peak power coefficient in order to mitigate fluctuations due to viscous effects and achieve realistic operation conditions. A high rotational speed ensures a high Reynolds number and therefore a low sensitivity to changes in the local flow conditions, while high centrifugal loads due to the rotational speed lead to a flap-wise blade bending moment when considering a coned rotor. Therefore, the selection of the used airfoil and the rotational speed of the rotor is driven by a compromise between airfoil thickness, which strongly influences the dependency of the airfoil characteristics on Reynolds number changes, and the Reynolds number itself. The SD7062 airfoil meets this requirements, as its thickness is 14 % and the drag coefficient as well as its sensitivity to changes in the Reynolds number is comparatively low. In order to realise a finite thickness at the trailing edge, the airfoil was cut at 96% of the chord length and then scaled to the original chord length again. To avoid undefined airfoil shapes due to an adjustment of the contours between two different airfoil geometries, only one airfoil shape is used over the blade radius. Similarly, the distributions of the chord length and twist (see table A1) form a compromise between a possibly high chord length, which directly contributes to the Reynolds number, and a high lift to drag ratio, which is necessary to achieve a high power coefficient. The considerations above lead to a rated rotational speed of 1200 RPM, a rated tip speed ratio of 6.25 and a local Reynolds number of 1.5×10^6 at the tip. Figure 1 shows a photograph of the blades mounted on the turbine. The local

Table 1: Model properties.

Rotor diameter	0.925 m
Rated wind speed	9.3 m/s
Rated rotational speed	1200 RPM
Nacelle diameter	72 mm
Tower diameter	57 mm
Distance blade tip to tower	530 mm
Distance rotor centre to coordinate system	80.6 mm
Air density	1.183 kg/m^3

Reynolds number, which is calculated from the free stream velocity and speed of the blade section, is maintained but decreases slightly until 30 % of the rotor radius and falls to 1.0 x 10^6 in the root region (see Figure 2). The rotation of the blades in combination with the cone angle induce extreme loads on the structure: At 0.5 R (radius), approximately 30 times the gravitational acceleration acts on the blade in the flap-wise direction. To withstand these accelerations, the blades were manufactured from a carbon fiber prepreg material, as an extremely lightweight and rigid material was demanded. A CNC-milled hard resistance foam core and a prepreg shear web were inserted into the blade and tempered together with the hull in an aluminium mould. Additionally, an aluminium part with threads at the blade root was inserted and aligned in the mould. Due to the high risk of undesired twisting, which may occur from the heating of the anisotropic material, it was necessary to conduct a 3D scan of the blades. Both blades showed a twist deviation below 0.2° from the original model. Additionally, a bending in flap-wise direction occurred with a magnitude below 0.3 % of the blade length at the blade tip. A second scan under operation-equivalent loading showed a higher flap-wise bending of approximately 0.6 % of the blade length but no significant bend-twist coupling.

The calibration of the sensor was carried out with 12 different load vectors in the expected field of operation to consider the effects of cross talking, as not only the aerodynamic loads but also high loads due to a small rotor imbalance are expected. The analysis of the calibration results shows that the expectable measurement uncertainty is 0.128 N in thrust, 0.024 Nm in torque, 0.008 Nm in yaw moment and 0.024 N in lateral force (with a confidence level of 95 %). In relation to the loads at rated conditions, a measurement uncertainty of 0.5 % in thrust and 2.3 % in torque and power is expected.

Different yaw angles from -55 to 55° were adjusted by an underfloor turntable with an uncertainty of below 0.25°. Two steps were conducted for the initial alignment of the 0° position: First, the rotor axis was aligned parallel to the wind tunnel floor using a digital level. Second, the blade tips were aligned with a line laser that projected a plane perpendicular to the wind tunnel floor and inflow direction. A maximum uncertainty of 0.5° is expected, as the wind tunnel floor cannot be assumed to be perfectly even.

All signals from the load cell were recorded over time and a low pass filter with a corner frequency of 40 Hz was applied. Extreme outliers were removed from the signal using a standard deviation-based filter. As the native coordinate system of the sensor is positioned on its top (see Figure 3), a coordinate transformation was applied. It was translated along the z-axis (perpendicular to the wind tunnel floor), such that the x-axis is equal to the rotor axis pointing in downwind direction. This transformation is based on the assumption that the lateral force on nacelle and rotor can be described as a single vector whose point of application lies on the rotor axis. This assumption seems reasonable as the nacelle is rotational symmetric. A further translation of the coordinate system into the rotor centre is not applicable

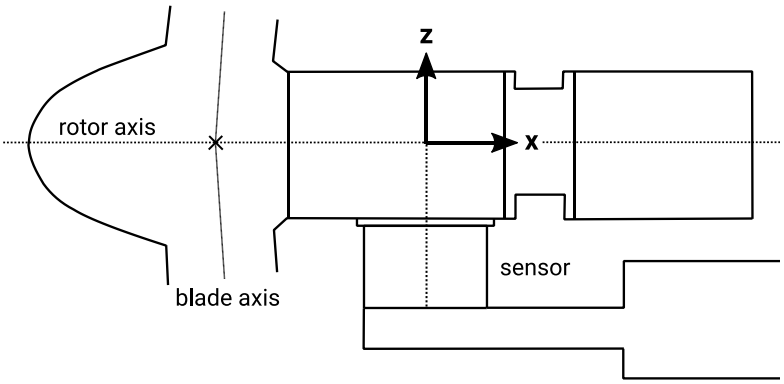

Figure 3: Sketch of the model turbine.

as the exact point of application of the lateral force in x-direction in unknown. Therefore, the origin of the coordinate system the presented loads refer to is located in a distance of 80.6 mm to rotor centre in downwind direction while the x-axis is identical to the rotor axis. Finally, a mean value was calculated for all signals in a window of 1 s, which corresponds to 20 rotor revolutions.

4. Results

Figure 4 illustrates the measured power, thrust and yaw moment coefficients as well as the lateral force of the model turbine at rated conditions (see table 1) and different yaw angles γ. A selection of the measured values can be found in table A2. The yaw angles range from -55 to 55° and are distributed symmetrically (apart from 3 points missing in the positive region). In sum, the measurements contain 54 different yaw angles. In the diagrams, black crosses connected with lines indicate the measurement points whereas blue crosses form the reflection of the measurement points at the y-axis. In case of the yaw moment, the blue crosses are additionally reflected at the x-axis in order to account for the change of the sign at the origin. Apart from the lateral force, all curves show a very smooth behaviour. When comparing the measurement points of power and thrust coefficients with their reflection, the differences are barely visible.

In Figure 4 (c), the yaw moment coefficient and the absolute yaw moment are shown on the primary and the secondary y-axis. The yaw moment coefficient is based on the idea of the thrust coefficient and is defined as follows:

$$C_{ym} = \frac{M_{yaw}}{1/2\,\rho v^2 A_{rotor} R_{rotor}}$$

Where M_{yaw} denotes the yaw moment with respect to the z-axis and air density, wind speed, rotor swept area and rotor radius are described by ρ, v, A_{rotor} and R_{rotor}, respectively. Analogous to the thrust coefficient, the denominator forms an ideal reference value, which is defined as the yaw moment arising from the maximum thrust force (referring to a thrust coefficient of 1) acting on a single blade tip when the blade is in a horizontal position. With this definition, the authors do not follow the suggestion of Kress et al. [6], as their definition depends on the blade surface rather than on the rotor swept area, which does not allow to compare two different rotor designs with respect to the yaw moment directly. The measured yaw moment can be described by a linear function with no offset and a slope of approximately 0.011 Nm per degree from -15 to 15°. With increasing yaw angle, the slope decreases until a maximum is reached between 37.5 and 40°. Comparing the measured values with their reflection at the y-axis, higher deviations as observed in torque and thrust occur. The lateral force shown in Figure

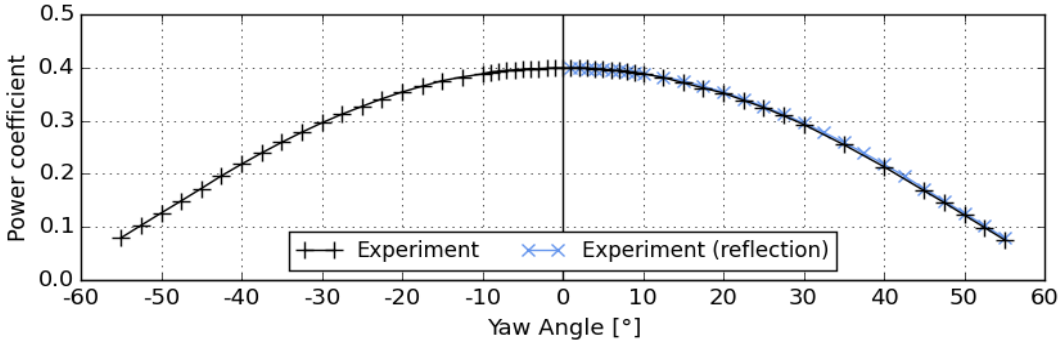

(a)

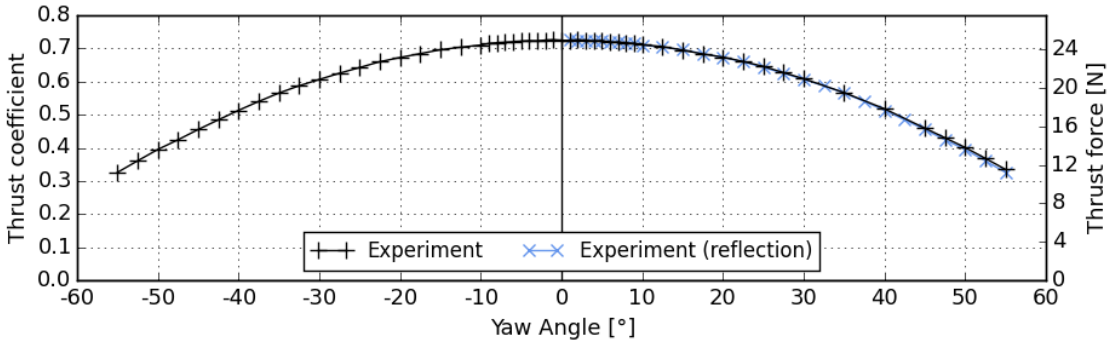

(b)

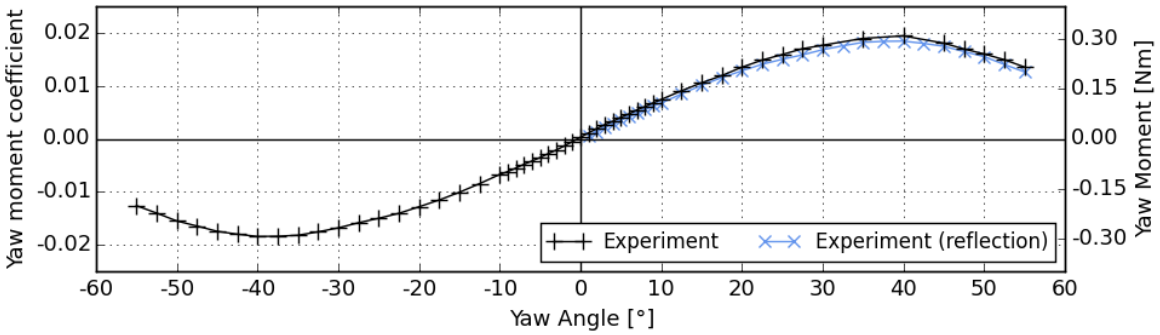

(c)

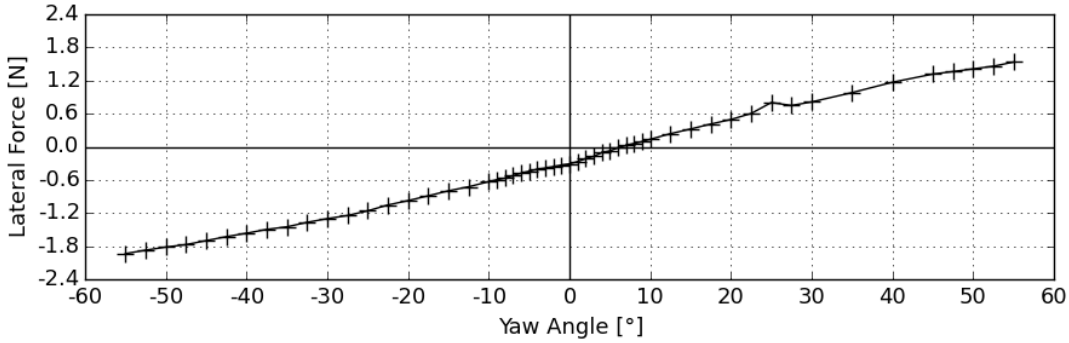

(d)

Figure 4: Experimental results for (a) power coefficient, (b) thurst coefficient, (c) yaw moment coefficient and (d) lateral force over yaw angle

4 (d) essentially behaves like a linear function even though the course of the curve is less smooth in comparison to the other quantities. A notable offset of approximately -0.3 N from the origin can be observed a 0° yaw angle. In comparison to the thrust force, the lateral force is small, which shows that the force acting on the rotor is aligned with the rotor axis but not with the wind direction. As the measurements contain forces on the rotor as well as on the nacelle, it is assumed that the main contribution of the lateral force arises from the nacelle drag force. However, the offset at 0° still cannot be explained in this way, as the drag force on the nacelle acting in the direction of the lateral force should be zero at this angular position.

When interpreting the results of the presented measurement campaign, it should be noted that although the experiments were carried out under controlled conditions in the wind tunnel, some uncertainties cannot be avoided and must therefore be taken into account. A systematic influence on the measurements is the contribution of the nacelle drag force to the yaw moment. As it is unknown at which position the resulting vector of the drag force on the nacelle is acting, the rotor yaw moment is superposed by a moment with a known force and an unknown lever arm. The mounting position of the nacelle on the sensor in x-direction is quite near to its centre, such that the lever arm can be assumed to be short in comparison to the nacelle length. Therefore, a deviation of the measured total yaw moment to the rotor yaw moment in a single-digit percentage must be considered when interpreting the results.

5. Summary and Conclusions

A description and analysis of the experimental study on a downwind coned, two-bladed rotor under yawed conditions was presented. The model description showed that a comparatively high and nearly constant Reynolds number over the blade span and an accurate manufacturing of the blades could be achieved. Results for thrust, power and yaw moment coefficients showed a symmetric and smooth behaviour over the yaw angle. In the course of the lateral force an offset was observed. The measured yaw moment is not fully equivalent to the rotor yaw moment. The reason for this is that the coordinate system used for the measurements is not located exactly in the centre of the rotor, but displaced in axial direction. Finally, no other significant uncertainties were observed in the measurement data.

A number of findings regarding the quality and results of the conducted experimental investigation based on the observations described in this work are elaborated below:

- The symmetry in the measured power and thrust coefficients as well as the zero crossing of the yaw moment at approximately 0° yaw angle confirms that the applied adjustment procedures were sufficient.
- The measurements clearly show that the direction of the rotor thrust force is aligned with the rotor axis but not with the wind direction, which sometimes leads to misunderstandings.
- When comparing the measured yaw moment to results of simulations, a careful analysis needs to be undertaken. On the one hand, the general shape and the characteristic point of maximum yaw can be compared with high accuracy. On the other hand, the absolute values may contain an uncertainty in a single-digit percentage.

As all relevant information needed for numerical simulations is given, this work offers a set of validation data open for all interested researchers. Special focus of this data set is the consideration of yaw moment, lateral force and a downwind coned rotor at different yaw angles. The authors therefore hope to contribute to the validation of current numerical models under yawed conditions.

Acknowledgments

The authors kindly thank the Federal Ministry for Economic Affairs and Energy of Germany (BMWi) for financially supporting the HyStOH project (03SX409A-F) and our partners Cruse Offshore GmbH, aerodyn engineering GmbH, JÖRSS –BLUNCK –ORDEMANN GmbH, DNV- GL and the Institute for Ship Structural Design and Analysis at the Hamburg University of Technology for the excellent cooperation.

Appendix

Table A1: Blade definition for 0° cone angle.

Radius [m]	Chord length [m]	Twist angle [°]	Twist centre [%]
0.046	0.050	-	50
0.066	0.050	-	50
0.090	0.130	19.94	27
0.115	0.126	17.02	27
0.140	0.116	14.10	27
0.165	0.101	12.11	27
0.190	0.089	10.13	27
0.215	0.080	8.88	27
0.240	0.072	7.63	27
0.265	0.066	6.99	27
0.290	0.061	6.35	27
0.340	0.052	5.48	27
0.390	0.046	5.02	27
0.440	0.042	4.46	27
0.465	0.040	4.00	27

Table A2: Measurement results for selected yaw angles.

Yaw angle [°]	Torque [Nm]	Thrust [N]	Yaw moment [Nm]	Lateral force [N]	Rotational speed [RPM]	Wind speed [m/s]
- 55	0.2018	11.22	-0.2014	-1.934	1204.87	9.271
- 50	0.3199	13.61	-0.2475	-1.816	1207.33	9.274
- 45	0.4382	15.69	-0.2787	-1.700	1203.67	9.277
- 40	0.5552	17.68	-0.2942	-1.565	1202.13	9.308
- 35	0.6578	19.48	-0.2905	-1.449	1205.78	9.293
- 30	0.7518	20.89	-0.2683	-1.301	1204.09	9.277
- 25	0.8291	22.13	-0.2394	-1.160	1205.97	9.302
- 20	0.9017	23.18	-0.2048	-0.975	1201.21	9.301
- 15	0.9556	23.98	-0.1611	-0.798	1201.58	9.342
- 10	0.9919	24.47	-0.1074	-0.632	1196.98	9.301
- 8	1.0004	24.70	-0.0882	-0.569	1201.98	9.253
- 5	1.0080	24.87	-0.0564	-0.442	1203.92	9.285
- 3	1.0120	24.91	-0.0339	-0.386	1201.40	9.288
0	1.0195	24.95	0.0046	-0.309	1198.30	9.274
3	1.0151	24.96	0.0427	-0.173	1202.56	9.297
5	1.0104	24.94	0.0648	-0.074	1203.75	9.319
8	1.0019	24.69	0.0972	0.061	1199.77	9.297
10	0.9884	24.50	0.1185	0.137	1203.19	9.335
15	0.9461	23.95	0.1686	0.323	1201.29	9.298
20	0.8950	23.22	0.2157	0.495	1204.07	9.298
25	0.8273	22.25	0.2539	0.802	1202.28	9.312
30	0.7465	20.97	0.2818	0.813	1201.22	9.290
35	0.6486	19.53	0.3024	0.982	1202.56	9.319
40	0.5402	17.84	0.3100	1.169	1209.34	9.297
45	0.4279	15.83	0.2879	1.317	1203.72	9.290
50	0.3104	13.82	0.2554	1.411	1208.27	9.316
55	0.1931	11.54	0.2161	1.534	1204.72	9.288

References

[1] Micallef D, Sant T 2016 A review of wind turbine yaw aerodynamics *Wind Turbines - Design, Control and Applications* (Intechopen)
[2] Hand M M, Simms D A, Fingersh L J, Jager D W, Cotrell J R, Schreck S, Larwood S M 2001 Unsteady Aerodynamics Experiment Phase VI: Wind Tunnel Test Configurations and Available Data Campaigns *Technical report* NREL
[3] Schepers G, Boorsma K, Cho T, Gomez-Iradi S, Schaffarczyk P, Jeromin A, … Sørensen, N N 2012 Analysis of Mexico wind tunnel measurements: Final report of IEA Task 29, Mexnext (Phase 1) *Technical report* ECN
[4] Maeda T, Kamada Y, Suzuki J, Fujioka H 2008 Rotor Blade Sectional Performance Under Yawed Inflow Conditions *Journ. of Solar Energy Engineering* **130**:1–7
[5] Adaramola M S, Krogstad P-Å 2011 Experimental investigation of wake effects on wind turbine performance *Renew. Energy* **36**:2078–2086
[6] Kress C, Chokani N, Abhari RS 2015 Downwind wind turbine yaw stability and performance. *Renew. Energy* **83**:1157–1165
[7] Koh J, Ng E 2016 Downwind offshore wind turbines: Opportunities, trends and technical challenges. *Renew. Sustain. Energy Rev.* **54**:797–808
[8] Schepers G, Snel H 2008 Model Experiments in Controlled Conditions - Final Report *Technical report* ECN
[9] Gómez-Iradi S, Steijl R, Barakos G N 2009 Development and Validation of a CFD Technique for the Aerodynamic Analysis of HAWT *Journ. of Solar Energy Engineering* **131**:1–13
[10] Sørensen NN, Michelsen J A, Schreck S 2002 Navier–Stokes Predictions of the NREL Phase VI Rotor in the NASA Ames 80 ft x 120 ft Wind Tunnel *Wind Energy* **169**:151–169
[11] Krogstad P-Å, Lund J A 2012 An experimental and numerical study of the performance of a model turbine *Wind Energy* **15**:443–457